Global Biogeochemical Cycles

RESEARCH ARTICLE
10.1029/2023GB007740

Processes in the Surface Ocean Regulate Dissolved Organic Matter Distributions in the Deep

Sarah K. Bercovici[1,2], **Thorsten Dittmar**[1,3], **and Jutta Niggemann**[1]

[1]Institute for Chemistry and Biology of the Marine Environment (ICBM), Research Group for Marine Geochemistry (ICBM-MPI Bridging Group), Carl von Ossietzky University of Oldenburg, Oldenburg, Germany, [2]National Oceanography Centre, Southampton, UK, [3]Helmholtz Institute for Functional Marine Biodiversity (HIFMB) at the University of Oldenburg, Oldenburg, Germany

Key Points:

- 70% of the molecular composition of dissolved organic matter (DOM) follows two-endmember water mass mixing in the deep Atlantic and Pacific
- There are small fractions of DOM with distinct chemical compositions that are added and removed relative to mixing
- Molecular formulae that behave conservatively in the deep are formed in the surface ocean and modified in overturning zones

Supporting Information:

Supporting Information may be found in the online version of this article.

Correspondence to:

S. K. Bercovici,
sarah.bercovici@uol.de

Citation:

Bercovici, S. K., Dittmar, T., & Niggemann, J. (2023). Processes in the surface ocean regulate dissolved organic matter distributions in the deep. *Global Biogeochemical Cycles*, *37*, e2023GB007740. https://doi.org/10.1029/2023GB007740

Received 16 FEB 2023
Accepted 24 OCT 2023

Author Contributions:

Conceptualization: Sarah K. Bercovici, Thorsten Dittmar, Jutta Niggemann
Data curation: Sarah K. Bercovici, Jutta Niggemann
Formal analysis: Sarah K. Bercovici, Thorsten Dittmar, Jutta Niggemann
Funding acquisition: Thorsten Dittmar, Jutta Niggemann
Investigation: Sarah K. Bercovici, Jutta Niggemann
Methodology: Sarah K. Bercovici, Thorsten Dittmar, Jutta Niggemann
Project Administration: Thorsten Dittmar, Jutta Niggemann

Abstract Marine dissolved organic matter (DOM) is a major global carbon pool, consisting of thousands of compounds with distinct lifetimes. While marine DOM persists for millennia, its molecular and isotopic composition imply that it is dynamic on shorter timescales. To determine the extent to which DOM deviates from conservative water mass mixing, we conducted a two-endmember mixing analysis on dissolved organic carbon (DOC) concentration and DOM molecular composition in the Atlantic and Pacific. Endmembers were the deep water masses near their formation sites. For DOM composition, we considered 6118 molecular formulae (MF) identified via Fourier-transform ion cyclotron resonance mass spectrometry in solid-phase extracts (SPE) of 837 samples. Bulk DOC and SPE-DOC concentrations behaved conservatively in both basins and ≥70% of the MF (14–20 μM SPE-DOC) mixed conservatively. However, a small fraction (10%–20%) of the MF (<3 μM SPE-DOC) were added or removed during mixing. These MF were more reduced and oxidized, respectively, than the conservative fraction. There were also MF absent from the endmembers; these accounted for ≤1 μM of SPE-DOC and positively correlated with DOM lability. Based on their distribution across the two basins, we conclude that the conserved MF are formed in the surface subtropical ocean and modified in overturning areas. In the deep ocean, however, these MF are solely controlled by mixing. This finding contrasts with the current paradigm of slow, continuous degradation of recalcitrant DOM in the deep ocean. Our analysis illustrates the importance of the surface ocean in controlling DOM cycling in the deep.

1. Introduction

At nearly 700 Pg C, the carbon reservoir of oceanic dissolved organic matter (DOM) rivals that of atmospheric CO_2 (Hansell et al., 2009). Most (>95%) of this reservoir resides in the deep ocean. The chemical components within DOM have distinct ages, reactivities and origins (Amon & Benner, 1996; Benner et al., 1997; Follett et al., 2014; Walker et al., 2016). Most DOM is produced photosynthetically in the surface ocean and introduced into the meso- and bathypelagic via physical processes such as deep convection (Carlson & Ducklow, 1996; Hansell & Carlson, 1998; Romera-Castillo, Letscher, & Hansell, 2016) and biogeochemical processes such as solubilization of sinking particles (Lopez & Hansell, 2021). Chemoautotrophy may constitute an in-situ source of DOM in the deep ocean (Hansman et al., 2009).

Past studies on DOM have conflicted regarding the extent to which it follows the mixing of deep water masses. Offsets in ^{14}C age between bulk dissolved organic carbon (DOC) and dissolved inorganic carbon (DIC) are consistent with the aging of water masses (i.e., conservative mixing) (Bercovici & Hansell, 2016; Bercovici, McNichol, et al., 2018; Druffel et al., 2016, 2021). The DOM composition in the North Atlantic is also primarily driven by mixing (Hansman, Dittmar, & Herndl, 2015). However, studies that separate DOM into specific fractions based on polarity or size reveal more dynamics within the DOM pool. Size and polarity fractions and even individual molecules within DOM have distinct radiocarbon ages, reactivities and origins (Broek et al., 2020; Follett et al., 2014; Lechtenfeld et al., 2014; Walker et al., 2016; Zigah et al., 2017). Ultrahigh-resolution mass spectrometry reveals that DOM contains hundreds of thousands of individual compounds (Zark, Christoffers, & Dittmar 2017), with structures that vary between deep ocean basins (Seidel et al., 2022). There are changes in DOC concentrations (Bercovici & Hansell, 2016; Hansell & Carlson, 1998) and DOM composition (Seidel et al., 2022) in water masses in the deep Atlantic to Pacific ocean basins, yet there is limited information as to what is driving these changes. In this study, we assessed the extent to which the molecular formulae within DOM follow mixing in the Atlantic, Southern and Pacific oceans. Our goal was to distinguish the fraction of molecular

Resources: Sarah K. Bercovici
Supervision: Thorsten Dittmar, Jutta Niggemann
Visualization: Sarah K. Bercovici
Writing – original draft: Sarah K. Bercovici
Writing – review & editing: Sarah K. Bercovici, Thorsten Dittmar, Jutta Niggemann

formulae within DOM that follow mixing from those molecular formulae that are added and removed relative to mixing.

We hypothesized that there is one fraction of DOM that behaves conservatively in the deep ocean on time scales of deep overturning and another fraction that slowly degrades and becomes molecularly modified. As DOM becomes more degraded, the proportion of CRAM (Hertkorn et al., 2006), the degradation index (Flerus et al., 2012) and the aromaticity index (AI_{mod}; (Koch & Dittmar 2006)) presumably increase, while the DOC concentration continuously declines over time. A previous study that assessed the molecular composition of DOM in crustal rocks west of the mid-Atlantic Ridge provided an in-situ representation of deep seawater left undisturbed for over 2000 years (Walter et al., 2018). That study found that not only did the DOC concentration decline over time, but the molecular composition of the DOM became more degraded. If there is indeed slow decay of DOM over time, we should be able to observe both its decrease in concentration and its chemical degradation along the ~1000-year transit from the North Atlantic to the far North Pacific.

1.1. Largescale Ocean Mixing

In the deep Atlantic Ocean, the two densest water masses are North Atlantic Deep Water (NADW) and Antarctic Bottom Water (AABW) (Schmitz, 1995; Talley, 2013). NADW is formed in the high latitude North Atlantic and is a mixture of subtropical surface waters and waters from the Arctic. NADW is distinguishable by its warmer temperatures (>2–10°C) and higher salinities (>34.7–34.9) compared to AABW (Figure 1). Upon NADW formation, DOM is downwelled to the deeper layers, elevating the DOC concentrations within NADW near its formation site (Fontela et al., 2016; Hansell & Orellana, 2021; Hansell et al., 2009).

Near the equator and into the Southern Ocean, NADW DOC concentrations are the same as in the other deep waters (Bercovici & Hansell, 2016), suggesting a loss of DOC in NADW during the decades between its formation to its transit to the northern subtropics (Fontela et al., 2020). Likewise, a recent modeling study (Matsumoto,

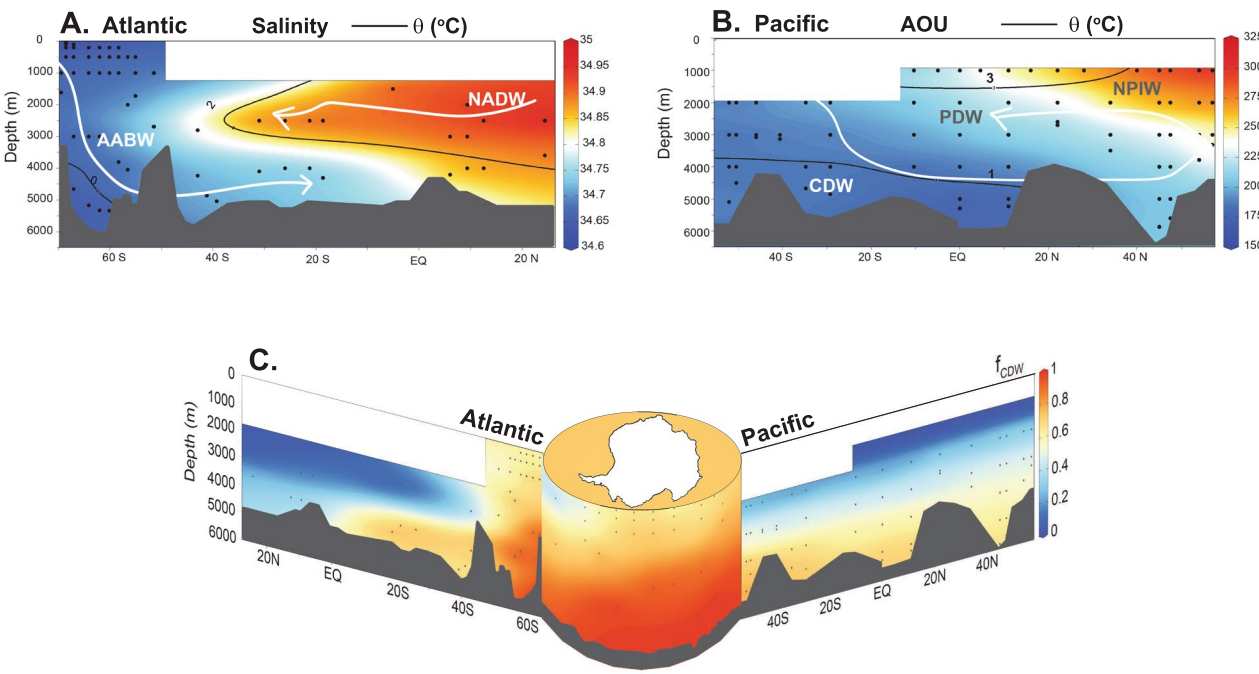

Figure 1. Latitudinal transects of (a)) the Atlantic, ANT28-4 and ANT 28-5 (sections outlined in Figure 2) and (b)) the Pacific oceans (SO248 and SO254; Figure 2), with salinity (in the Atlantic) or apparent oxygen utilization (AOU; in the Pacific) in color, with potential temperature (θ) in contours. AOU is depicted in color in the Pacific transect (b) because it clearly distinguishes NPIW and PDW from CDW. Subpanel C combines panels (a and b) for a global view at the fraction of CDW (AABW in the Atlantic), calculated using salinity and potential temperature. White boxes cover the areas that are not controlled by the deep-water mass mixing considered in this analysis. Surface data are present in the Atlantic Sector of the Southern Ocean because there CDW (AABW) reaches up to 200 m depth. Sections were plotted using Ocean Data View (Schlitzer, 2023).

Tanioka, & Gilchrist, 2022) reported that the steepest DOC concentration gradient in the deep global ocean occurs in the Atlantic basin.

AABW is the densest water mass in the open ocean and is formed in the Southern Ocean. It is a mixture of NADW, deep waters from the Pacific and Indian oceans, and exported Antarctic shelf waters that all mix in the Antarctic circumpolar current (Talley, 2013). AABW is characterized by its cold temperatures (0°C) and flows northward from the Southern Ocean, filling all major ocean basins (in the Pacific, the deep waters from the Southern Ocean are referred to as the lower Circumpolar Deep Water fraction; CDW; Figure 1).

In the Pacific, CDW flows northward. When CDW reaches high northern latitudes (>40 N), it upwells and entrains North Pacific Intermediate Water (NPIW). This overturning forms the moderately dense Pacific Deep Water (PDW), which then migrates southward. PDW is most clearly distinguished by its relatively higher apparent oxygen utilization (AOU > 200 μM; Figure 1b). In this study, we apply a simple deep water mixing model for each ocean basin to the molecular formulae (and their relative FT-ICR-MS signal intensities) identified in our largescale DOM dataset to identify the extent to which the individual formulae follow deep mixing. We use this mixing approach with molecular formulae measured in the linear range of the FT-ICR-MS, in which signal intensities correlate linearly with respect to mixing (Seidel et al., 2015).

2. Methods

2.1. Sample Collection

Samples for DOM composition in the Atlantic Ocean and Atlantic sector of the Southern Ocean were collected on three cruises aboard the *R.V. Polarstern*: ANT-XXVIII/2, ANT-XXVIII/4, and ANT-XXVIII/5, and from the Bermuda Atlantic Time Series (BATS) station aboard the *R.V. Atlantic Explorer* (Figure 2). Samples for DOM composition in the Pacific Ocean and Pacific sector of the Southern Ocean were collected on three cruises aboard the *R.V. Sonne*: SO245, SO248, and SO254, and from the Hawaii Ocean Time-series (HOTS) station aboard the *R.V. Kilo Moana* (Figure 2). Full water column profiles were collected from a rosette of Niskin samplers equipped with conductivity, temperature and depth sensors. This analysis includes 364 samples from the Atlantic and 473 samples from the Pacific (Figure 2). All data reported here is published and open access at PANGAEA® Data Publisher (Bercovici et al., 2023). The bulk DOC concentration data considered in the analysis are from a publicly available compilation (Hansell et al., 2021).

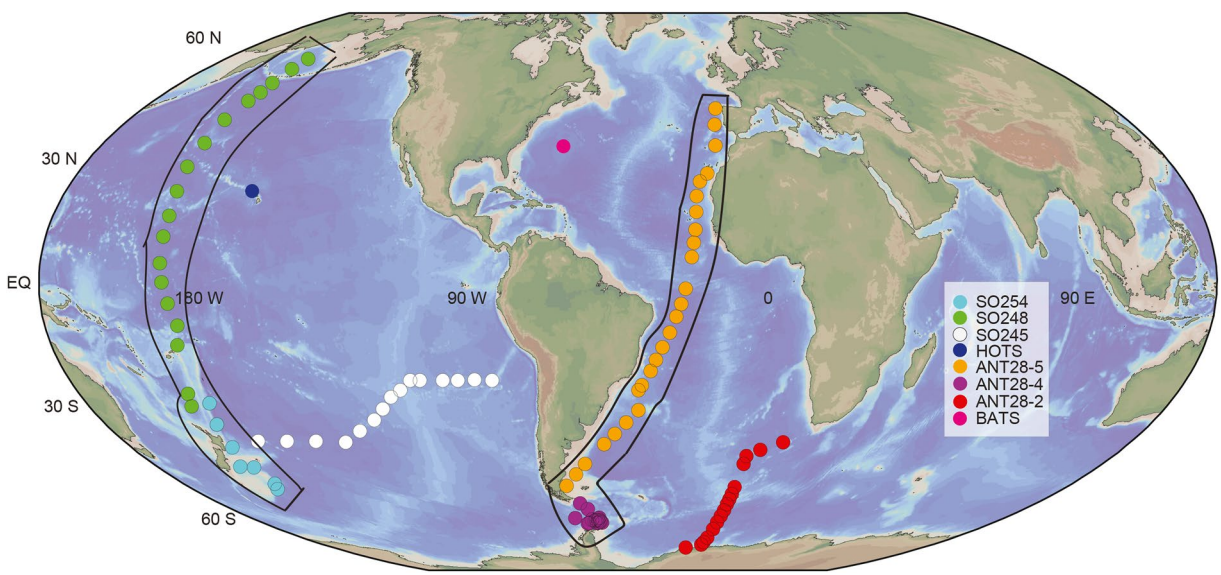

Figure 2. Global map of stations (plotted with Ocean Data View; Schlitzer, 2023). The black frames on ANT28-4 and ANT28-5 and SO248 and SO254 represent the data visualized in the U-shaped plots in Figures 1c and 5.

2.2. Solid Phase Extraction and DOC Quantification

Samples for DOM composition analysis were extracted via the solid-phase extraction (SPE) method (Dittmar et al., 2008). In short, 4 L of seawater were filtered through a pre-combusted (400°C, 4 hr) 0.7 µm glass fiber filter (GF/F, Whatman, United Kingdom) and acidified to a final pH of 2 (HCl, 25%, p.a., Carl Roth, Germany). We collected 4 L of seawater for SPE to ensure that we extracted enough DOM (in terms of carbon), even when considering the low DOC concentrations in the deep ocean (35–40 µM). Samples were extracted on commercially pre-packed cartridges (1 g PPL, Agilent, USA) via gravity flow. After extraction, the cartridges were rinsed with two volumes of ultrapure water (pH 2) and subsequently dried with nitrogen gas. The DOM was then eluted from the cartridges with 6 ml of methanol (HPLC-grade, Sigma-Aldrich, USA) into pre-combusted amber glass vials. These DOM extracts were stored in the dark at −20°C until FT-ICR-MS (Fourier-transform ion cyclotron resonance mass spectrometry) analysis.

For the determination of SPE-DOC concentrations small aliquots (100 µL) of the solid-phase extracts were dried in a stove at 50°C overnight, redissolved in 10 mL ultrapure water and analyzed on a Shimadzu TOC-VPCH total organic carbon analyzer. Under consideration of extraction and elution volumes, measured concentrations were converted to concentrations in seawater. Bulk DOC was determined directly on the same analytical instrument. The solid-phase extraction efficiency is the ratio between SPE-DOC and bulk DOC concentrations. The DOC analyses were quality controlled using the consensus reference material for DOC concentration provided to the community by the Hansell Biogeochemistry Laboratory (University of Miami, Miami, FL, USA; CV = 5%). The mean extraction efficiency of all Atlantic samples was 58 ± 6%, similar to the extraction efficiency of the reference DOM material from the deep North Pacific (61 ± 3%; (Green et al., 2014)). Unfortunately, DOC samples from our Pacific transects were partially contaminated with volatile organics, so we were unable to use them to calculate extraction efficiencies. SPE-DOC samples were unaffected by any contamination. This study focusses on SPE-DOC because it is the analytically attainable fraction for molecular DOM characterization via FT-ICR-MS.

2.3. Molecular Composition of DOM

All DOM extracts were analyzed on a SolariX XR FT-ICR-MS (Bruker Daltonik GmbH, Bremen, Germany) equipped with a 15 T superconducting magnet and an electrospray ionization source (ESI; Bruker Apollo II ion source). For analysis, all DOM extracts were mixed with ultrapure water and methanol (MS grade, 1:1 v/v) to a final carbon concentration of 2.5 ppm. For analysis validation, an in-house DOM reference sample, collected at the Natural Energy Laboratory of Hawaii Authority in 2009 (Green et al., 2014), was measured twice a day.

FT-ICR-MS was performed in ESI negative ion mode, with a voltage of 4.5 kV, flow rate of 360 µL/hr, temperature of 200°C and hexapole accumulation time of 0.65 ms. Samples were injected using an autosampler (CTC Analytics AG, Zwingen, Switzerland) and 200 scans were accumulated per sample in a mass window ranging from 92 to 1000 Da. All spectra were calibrated internally using Bruker Daltonik Data Analysis software and processed using ICBM-OCEAN (Merder et al., 2020) that includes a series of validation steps for further mass calibration, peak matching between samples and molecular formula assignment (see supplement for detailed settings). Only the most abundant isotopologues (^{12}C, ^{14}N, ^{16}O etc.) were considered for our largescale data interpretation in an oceanographic context. The weighted means and standard deviations of the O/C and H/C ratios were calculated using the "stat" and "radiant" packages in R. The Shannon and functional diversity indices were calculated following the methodology described in Mentges et al. (2017). The Molecular Lability Boundary (MLB) was defined in D'Andrilli et al. (2015). The MLB divides the molecular constituents of DOM into more and less labile groups based on H/C ratios (where H/C > 1.5 for more labile DOM), providing a simple method to estimate the lability of DOM across a variety of different environments.

2.4. Mixing Model Setup

Two end-member mixing of deep water masses was assessed with salinity and potential temperature. First, we binned data from the endmembers using their physicochemical characteristics (Figure 1; Table S1 in Supporting Information S1). Newly produced NADW was characterized as those data in the high latitude North Atlantic with potential density values >27.7 kg m^{-3}, potential temperatures between 2 and 4°C, and salinities >34.6 (Figure 1; (Schmitz, 1995)). Newly produced AABW and CDW were characterized as those data south of the polar front (>50°S), where potential density values were also >27.7 kg m^{-3}, salinities were >34.6 and <34.75, and potential temperatures were ≤0°C. NPIW was characterized in the far North Pacific, where potential temperature was <4°C and AOU was >300 μM (Figure 1).

Then, we generated the mixing model equations, in which every datapoint in the deep ocean was simply a component of the two endmembers. Since salinity and θ are conserved variables in the deep ocean, the salinity and θ for a given sample would be as follows:

$$\mathrm{Sal} = \mathrm{Sal}_A * f_A + \mathrm{Sal}_B * f_B \quad (1)$$

$$\theta = \theta_A * f_A + \theta_B * f_B \quad (2)$$

where f_A and f_B are the fractions of each water mass of interest (either NADW and AABW, or NPIW and CDW), and Sal_A, Sal_B, θ_A, and θ_B are the salinities and potential temperatures of each water mass endmember. Sal and θ are the salinity and potential temperature data in each sample where we are applying the model. To solve for each fraction f_A and f_B, the two equations can then be re-arranged as follows:

$$f_A = \left[(\mathrm{Sal}_B * \theta) - (\mathrm{Sal} * \theta_B)\right] \Big/ \left[(\theta_A * \mathrm{Sal}_B) - (\mathrm{Sal}_A * \theta_B)\right] \quad (3)$$

$$f_B = 1 - f_A \quad (4)$$

The modeled, conserved DOM composition was then calculated, assuming it behaves like a conservative variable (like salinity or θ):

$$\mathrm{DOM}_C = f_A * \mathrm{DOM}_A + f_B * \mathrm{DOM}_B \quad (5)$$

where DOM_C is a conserved DOM composition and DOM_A and DOM_B are the DOM compositions for each endmember. We isolated the water masses based on the purest possible endmembers in our dataset, based on proximity to water mass formation site and physical characteristics (Figure 1). The endmembers were averaged from 3 pure NADW samples, 12 pure AABW samples, 22 pure CDW samples and 6 pure NPIW samples to determine DOM_A and DOM_B. Any molecular formulae whose peak intensity fell below the method detection limit after averaging was removed. It should be noted that the NADW endmember here is NADW in the subtropics that has already existed for several decades. Both the data analysis and the model setup were conducted in R Programming Language (2022).

A conserved dataset was calculated as the fraction of each water mass for each sample multiplied by the relative peak intensity of each molecular formula within each water mass endmember. We then correlated the modeled dataset of every sample in with the observed counterpart, isolated at potential density (σ_θ) values > 27.7 kg m^{-3} to only consider the abyssal water masses that are primarily controlled by simple mixing.

We then separated the molecular formulae into groups based on whether they followed the mixing model or were added or removed relative to mixing. We estimated the DOC concentration of each group by multiplying the proportion of total peak intensity of all molecular formulae in each group of each sample by their respective SPE-DOC concentrations (Figure S1 in Supporting Information S1). Because the DOM fractions are defined as specific groups of molecular formulae captured in SPE-DOC, estimated concentrations give the DOC contributed by the identified groups.

3. Results

3.1. Physical Characteristics, DOC Concentration, and DOM Composition of the Endmembers

Salinity and potential temperature (θ) values of each water mass endmember are reported in Table S1 in Supporting Information S1. NADW was the most saline (salinity of ~35) and warmest water mass (2.8 ± 0.1°C), while AABW and CDW were fresher (salinities of ~34.65) and colder (<0°C). NPIW had θ values of ~2.7°C and was fresher (salinity of ~34.3) than the other endmembers. The SPE-DOC concentrations of the endmembers in each mixing model were similar, although the Atlantic endmembers had slightly higher SPE-DOC concentrations than those in the Pacific (Table S1 in Supporting Information S1). In total, there were 6118 detected molecular formulae in our dataset, with >50% of them present in the water mass endmembers of our mixing models. All water masses in this mixing analysis shared 2731 molecular formulae (Figure S2a in Supporting Information S1) that comprised 79% of the total number of molecular formulae in all endmembers and ≥90% of the total peak intensity in each sample. There were 741 molecular formulae that were not present in every endmember, with 452 molecular formulae shared by at least two water masses, and 289 unique to one water mass (Figure S2a in Supporting Information S1). All water masses had similar richness (number of molecular formulae), O/C and H/C ratios, as well as abundance-based (Shannon) and functional (Mentges et al., 2017) diversity applied to the H/C ratios (Table S1 in Supporting Information S1). The functional diversity provides information on the range of H/C ratios and how that differs between samples. It therefore provides an estimate of how diverse the chemical properties are within a given sample. All these chemical and diversity parameters indicate that the abundance and distribution of molecular formulae were similar between all water masses.

3.2. Mixing Model Results

We first conducted the mixing model on bulk DOC concentrations (Hansell et al., 2021) tracking the same geographic extent as our dataset to determine if bulk DOC behaves the same as the SPE-DOC in our dataset. When conducting the mixing model (Equation 1) on bulk DOC concentrations (Hansell et al., 2021) with the same latitudinal range as our data, the observed and modeled bulk DOC values in the deep Atlantic (2500 samples considered) were 40 ± 1 μM and 40.3 ± 0.3 μM, respectively. Mean observed and modeled bulk DOC values in the deep Pacific (11,046 samples considered) were 39 ± 2 μM and 39 ± 1 μM, respectively. The anomalies were 0 ± 1 μM in the Atlantic and 0 ± 2 μM in the Pacific.

In this study, we analyzed 110 samples in the deep Atlantic and 162 samples in the deep Pacific water masses, respectively (here deep is defined as $\sigma_\theta > 27.7$, and would thus only include NADW, AABW, CDW, and PDW). The observed and modeled SPE-DOC values in the deep Atlantic were 25 ± 4 and 24 ± 1 μM, respectively (1 ± 4 μM anomaly, calculated as the difference between observed and modeled values, where the error is propagated from the standard error in SPE-DOC concentrations of each water mass). In the deep Pacific, observed and modeled values were 22 ± 5 μM and 22 ± 2 μM, respectively (1 ± 5 μM anomaly, where the error is propagated from the standard error in SPE-DOC concentrations of each water mass).

The observed DOM molecular composition generally fit well with the modeled counterpart, with R^2 values ranging from 0.729 to 0.998 (0.96 ± 0.05) (example in Figures S2b and S2c in Supporting Information S1). As the R^2 values between observed and modeled DOM composition indicate how well one sample follows mixing, those samples with a lower R^2 value are indicative of non-conserved processes in the deep-water column. The goodness of fit of the model was inversely related to the Molecular Lability Boundary (MLB: (D'Andrilli et al., 2015)), which is defined as those molecular formulae with H/C ratios >1.5 and is used to estimate the lability of DOM (in other words: the higher the proportion of molecular formulae with H/C > 1.5, the more labile the DOM). The MLB and the R^2 values of the model had an inverse correlation (Figures 3a and 3b; $R^2 = 0.84$, $p < 0.0001$ for the Atlantic, $R^2 = 0.80$, $p < 0.0001$ for the Pacific).

We next separated out the group of molecular formulae whose FT-ICR-MS signal intensities fell on a 1:1 line with the mixing curve from those that deviated from the 1:1 line with >99% confidence (based on a z score of 3. The standard deviation was 3×10^{-4} for the Atlantic and Pacific mixing curves, respectively; Figure S2c in Supporting Information S1). We defined these groups (definitions described in Figure S2c in Supporting Information S1) as:

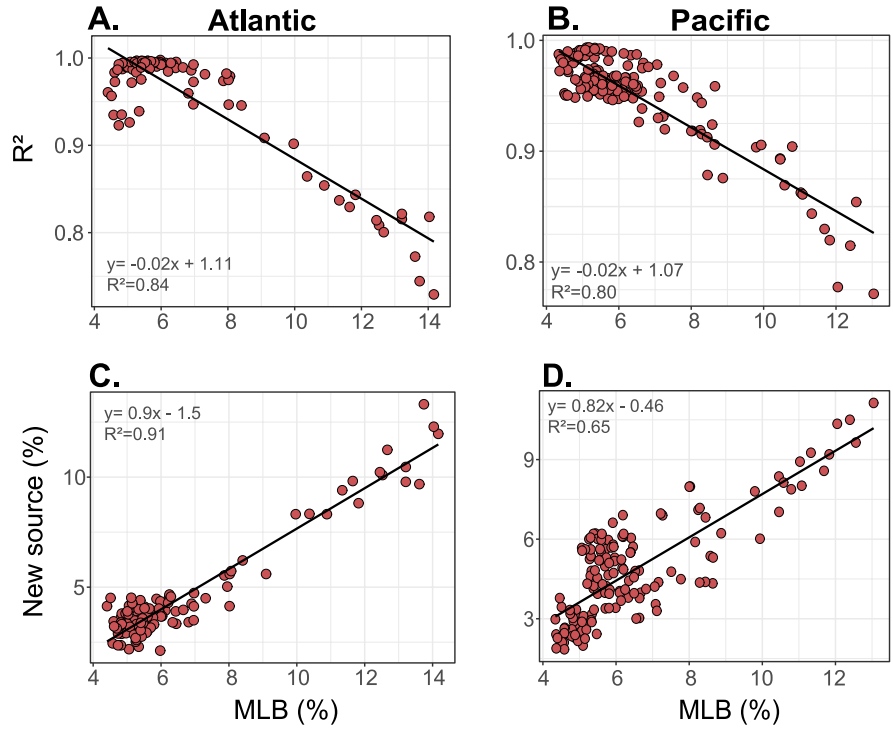

Figure 3. (a and b) R^2 values of the mixing model and (c and d) percent signal intensity of the *new source* molecular formulae versus the MLB (defined as H/C > 1.5) for the Atlantic (lefthand plots) and Pacific (righthand plots). Each dot represents a seawater sample.

- *Core*: molecular formulae that follow mixing with 99% confidence.
- *Sink*: molecular formulae present in the endmembers that either decreased in abundance relative to the mixing curve or were removed entirely.
- *Existing Source*: molecular formulae present in the endmembers that increased in peak intensity relative to mixing.
- *New Source*: molecular formulae not detected in the two endmembers but present in the mixed sample.

The *core*, *sources*, and *sink* groups have distinct compositions regarding the presence and signal intensities of molecular formulae (Figures 4 and 5; Table 1).

3.2.1. The Core Group: Molecular Formulae That Follow Mixing

The *core* group made up 72%–81% of the total peak intensity of every sample in each ocean basin (Table 1) and followed simple mixing in the deep ocean with >99% confidence. It mostly consists of highly unsaturated, oxygen-poor compounds (60% of the peak intensity of molecular formulae in the Atlantic and Pacific; Figure 5). The core also contains a substantial proportion of unsaturated, oxygen-rich molecules (approximately 30% the relative peak intensity of the Atlantic, and Pacific, respectively). The mean O/C and H/C ratios of the core (Table 1) match those of carboxylic-rich alicyclic molecules (CRAM, (Hertkorn et al., 2006)) and the "Island of Stability" (H/C = 1.3 ± 0.2 and O/C = 0.5 ± 0.1; Lechtenfeld et al., 2014).

3.2.2. The Sink: Molecular Formulae Removed Relative to Mixing

While the *sink* comprised only 46–69 molecular formulae, it made up ~6–18% of the total peak intensity in all samples. The *sink* chemical composition includes highly unsaturated, oxygen-rich compounds (90% in the Atlantic and 72% in the Pacific) and highly unsaturated, oxygen-poor compounds (10% in the Atlantic and 28% in the Pacific; Figure 5). The *sink* group was more oxidized in comparison to the *existing source* and exhibited higher O/C and O/H ratios than the other groups (Figures 4c and 4d, Table 1).

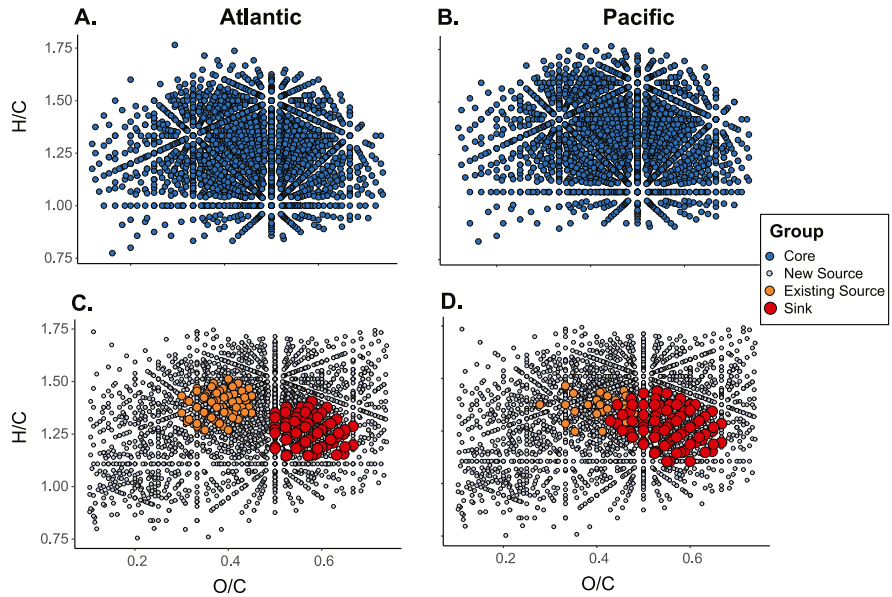

Figure 4. Van Krevelen plots for (a and b) the *core* and (c and d) the *sources* and *sink* groups in the Atlantic (lefthand plots) and Pacific (righthand plots).

3.2.3. Existing Source: Molecular Formulae Added Relative to Mixing

The *existing source* group consisted of only 23–60 molecular formulae but made up ~3–15% of the total peak intensity in the deep DOM samples (Table 1). This group is dominated by highly unsaturated, oxygen-poor compounds in the Atlantic and Pacific oceans (97% and 100%, respectively; Figure 4). In the Atlantic, the *existing source* also contains a small proportion (3%) of unsaturated oxygen-poor components.

3.2.4. New Source Molecular Formulae

The *new source* group of molecular formulae had the most diverse chemical assembly of all groups (Figure 5) yet made up only ~2–13% of the total peak intensity (Table 1). The relative proportion of the *new source* group had a positive correlation with MLB in both oceans ($R^2 = 0.91$ and 0.65 in the Atlantic and Pacific, respectively; Figures 3c and 3d). Samples contained between 244 and 1294 molecular formulae identified in the *new source* group (median of 590 molecular formulae). Moreover, only 9%–20% (293 in the Atlantic and 749 in the Pacific) of all *new source* molecular formulae (3331 in the Atlantic and 3294 in the Pacific) were present in more than half of the samples, implying high variability between samples. The chemical composition of the *new source* group was similar in each ocean basin: it consists of ~10% aromatics, ~40% highly unsaturated oxygen poor, 25% highly unsaturated oxygen rich, ~18% unsaturated; 7% of the unsaturated compounds contained nitrogen. Most aromatic molecular formulae present in the sample set were identified in the *new source* group (Table 1).

4. Discussion

4.1. DOC Concentrations Follow Mixing in the Deep Atlantic and Pacific

In the North Atlantic, there is a loss of bulk DOC from the high latitude formation of NADW to the northern subtropics, bringing the DOC concentrations from ~48 to ~40 μM (Bercovici & Hansell, 2016; Fontela et al., 2016; Matsumoto, Tanioka, & Gilchrist, 2022). From that point, DOC concentrations remain ~40 μM until deep waters well up in the Southern Ocean, mix with other waters, and are influenced by surface and Antarctic shelf biogeochemistry. In the Pacific, DOC concentrations are several μM lower (~37 μM; (Hansell et al., 2009)). The mixing model (Equation 4) on bulk DOC concentrations (Hansell et al., 2021) with the same

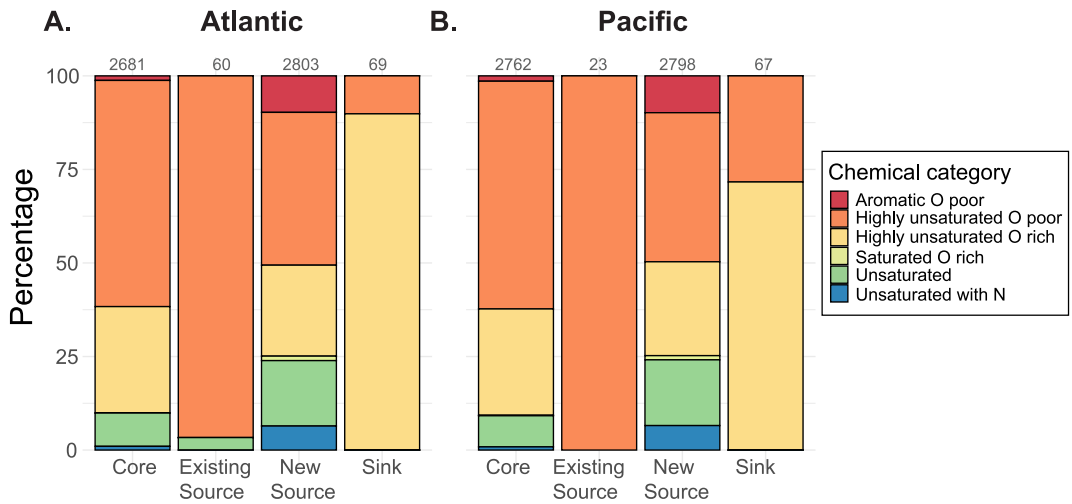

Figure 5. Bar plots depicting the chemical categories of (a) the Atlantic and (b) Pacific data. Categories are based on molecular formulae and were obtained with ICBM-OCEAN (Merder et al., 2020). The numbers above the bar plots represent the number of molecular formulae belonging to each group.

latitudinal range as our data, suggests that DOC behaves conservatively in both the Atlantic and Pacific deep ocean basins.

This study is based on SPE-DOC, which is analytically accessible for molecular DOM characterization via FT-ICR-MS and is well defined and highly reproducible (Dittmar et al., 2008; Green et al., 2014). There is not a substantial ^{14}C age difference at depth between bulk and SPE-DOC (Broek et al., 2017), implying that general DOM characteristics in the deep ocean basins are well represented by PPL-extracted DOM. To determine if SPE-DOC behaved the same way as bulk DOC, or whether there is a fraction not captured by SPE-DOC that behaves non-conservatively in the deep ocean, we conducted the mixing model on SPE-DOC and on the total DOC concentrations. While we never directly compare the bulk DOC concentrations with our DOM composition dataset, we find that with two endmember mixing, deep SPE-DOC and deep DOC both behave conservatively.

Our mixing analysis with SPE-DOC concentrations showed that while they behave conservatively in their respective deep ocean basins, there is a loss of SPE-DOC from the Atlantic to the Pacific (Figure 6a). This loss in concentration is consistent with respective trends in bulk DOC concentrations and apparent ^{14}C ages from

Table 1
Number of Identified Molecular Formulae (N), Their Total Peak Intensity (%), Average (±SD) for m/z, O/C, H/C and O/H Ratios, and the Peak Intensity (%) of Aromatic Compounds for Those Molecular Formulae in the Core, Existing Source, New Source and Sink Groups in the Deep Atlantic and Pacific Oceans

	N	Total peak intensity (%)	m/z	O/C	H/C	O/H	Aromatics (%)
ATLANTIC (5521)							
Core	2,681	70 ± 1	445 ± 114	0.5 ± 0.1	1.3 ± 0.2	0.4 ± 0.1	1.2
Ex. Source	60	11 ± 1	386 ± 4	0.38 ± 0.04	1.35 ± 0.08	0.28 ± 0.03	0
New Source	2,803	4 ± 2	478 ± 141	0.5 ± 0.1	1.3 ± 0.2	0.4 ± 0.1	8.3
Sink	69	13 ± 3	439 ± 45	0.57 ± 0.05	1.19 ± 0.08	0.48 ± 0.06	0
PACIFIC (5693)							
Core	2,762	76 ± 2	444 ± 113	0.5 ± 0.1	1.3 ± 0.2	0.4 ± 0.1	1.4
Ex. Source	23	3.1 ± 0.4	450 ± 95	0.41 ± 0.05	1.32 ± 0.07	0.31 ± 0.04	0
New Source	2,798	5 ± 3	475 ± 142	0.4 ± 0.1	1.3 ± 0.2	0.4 ± 0.1	8.5
Sink	67	14 ± 3	415 ± 38	0.55 ± 0.06	1.2 ± 0.1	0.45 ± 0.07	0

Note. The total number of molecular formulae for each deep ocean basin is listed next to the ocean label.

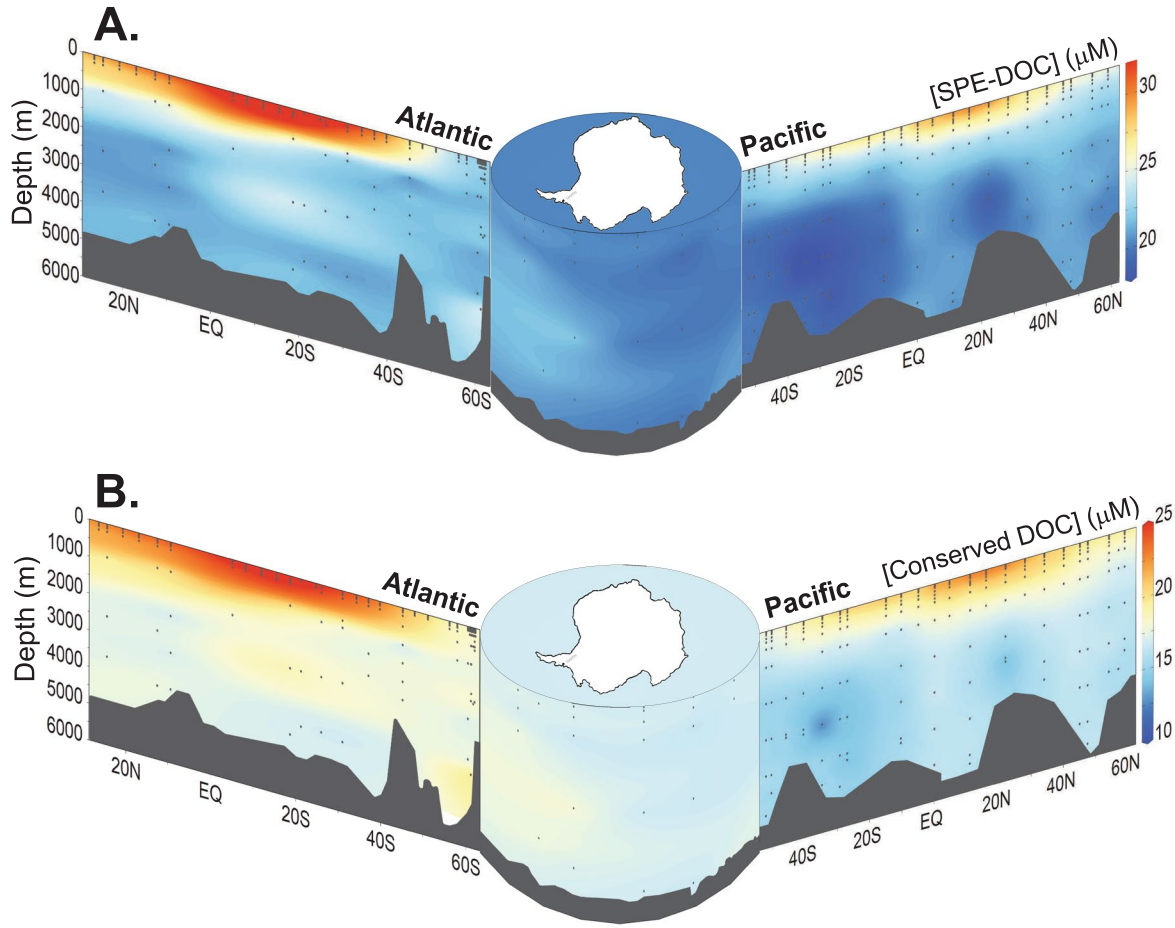

Figure 6. Latitudinal cross-section plots of the Atlantic (lefthand section plots), the Southern Ocean and the Pacific (righthand section plots; sections outlined in Figure 2) of (a) the total SPE-DOC concentration and (b) the conserved DOC concentration. The conserved DOC concentration is calculated from multiplying the percent total peak intensity of the *core* molecular formulae by the SPE-DOC concentration. Note that the definition of the *core* was derived from deep water masses only. The classification into *core* molecular formulae was done here also for surface samples. Sections were plotted using Ocean Data View (Schlitzer, 2023).

the South Atlantic to the South Pacific. The bottom waters exported from the Southern Ocean into the Pacific notably have lower DOC concentrations and older apparent ^{14}C ages (34–37 μM, ~6000 ^{14}C years; (Druffel & Griffin, 2015) than the deep waters entering the Southern Ocean from the Atlantic sector (40 μM, ~5,000 ^{14}C years; (Druffel et al., 2016)).

Like DOC and SPE-DOC concentrations, most (73 ± 4%) of the DOM constituents followed conservative, 2-endmember mixing and were therefore classified in the *core* group. However, there were *sources* and *sink* molecular formulae in every DOM sample that behaved dynamically on the considered timescales of ocean circulation and are distinguishable by their composition (Figures 4 and 5).

4.2. Occurrence of the Core, Source and Sink Groups Is Linked to Chemical Composition

The *core* group of molecular formulae has a chemical makeup similar to published DOM compositions from the deep Atlantic and Pacific oceans (Hansman, Dittmar, & Herndl, 2015; Medeiros et al., 2015; Osterholz et al., 2021). It has a high proportion of highly unsaturated compounds (Figures 4 and 5), which are most likely microbially degraded photosynthetic products that make up a large portion of all marine DOM (Medeiros et al., 2015). It is remarkable that deep water masses originating from distinct regions share such similar DOM chemical composition. This result is likewise observed in Hansman et al. (Hansman, Dittmar, & Herndl, 2015), who found no water mass-specific DOM composition and that all samples from the investigated area in the northeast Atlantic Ocean,

regardless of depth and latitude, shared 96% similarity. Moreover, Lechtenfeld et al. (2014) identified the "Island of Stability," a group of molecular formulae within CRAM (Hertkorn et al., 2006) that hold a high residence time and are abundant and ubiquitous in both the deep Atlantic and Pacific oceans (Bercovici, Koch, et al., 2018). Past reports suggest that the similarity in composition is also true on a structural level (Zark & Dittmar 2018). However, recent work using nuclear magnetic resonance spectroscopy reports structural differences in DOM between different water masses (Seidel et al., 2022). These studies imply both universal and variable fractions in deep-sea DOM in all major ocean basins.

Every sample contained molecular formulae in the *new source* group. The higher proportion of unsaturated and N-containing compounds is consistent with increased contributions of molecular formulae related to more labile compounds such as peptides and amino sugars (Figure 5; Schmidt et al., 2009). Moreover, the positive correlation of these molecular formulae with the MLB (D'Andrilli et al., 2015), implies that the *new source* group is more bioavailable than the other groups (Figure 3). As the *new source* fraction is not controlled by simple mixing, it is likely introduced into the deep ocean by export or advection of fresh material from the surface or by in situ microbial processing or chemoautotrophy (Hansman et al., 2009). While the *new source* group was present everywhere in the ocean at low concentrations, its high variability between samples suggests a fast turnover and renewal on timescales much smaller than mixing.

The group of *existing source* molecular formulae also had a distinct chemical composition (Figures 4 and 5). Both the large contribution of highly unsaturated oxygen-poor compounds to this group, and its similar O/C and H/C ratios compared to CRAM (Figures 4c and 4d), suggest that this group is more refractory than the *new source* group. The *existing source* group could be a product of continuous microbial reworking and degradation of more labile DOM (Dittmar et al., 2021), as suggested by the microbial carbon pump concept, in which labile DOM is microbially reworked thereby becoming more refractory (Jiao et al., 2011). These more recalcitrant molecular formulae are not efficiently degraded by the deep microbial communities, they therefore are both added to the system relative to mixing and are in the mixing endmembers. However, as the *existing source* molecular formulae do not accumulate along deep-water mass transit, they appear to be at a steady state and therefore are likely degraded when their concentration reaches above a certain threshold.

The molecular formulae removed relative to mixing were distinctly different compared to those of the other groups. This group was dominated by highly unsaturated oxygen-rich compounds. Highly oxidized components of DOM are more susceptible to removal via abiotic processes such as sorption or gel formation (Avneri-Katz et al., 2017; Verdugo, 2004). Moreover, gels coagulate via carboxyl group interactions, which are directly correlated with the O/H ratio in a sample (Zark, Christoffers, & Dittmar 2017). The *sink* group has a higher O/H ratio than the other groups (Table 1), suggesting that this group would be more susceptible to aggregation and subsequent removal from the water column.

4.3. Conserved DOM Behavior in the Global Ocean

The global distributions of the SPE-DOC concentrations (Figure 6a) followed the same pattern as the total DOC concentrations in the Atlantic and Pacific Oceans (Hansell et al., 2009), where surface DOC concentrations are higher in the subtropical gyres and equator and lower at high latitudes. We multiplied the relative peak intensity of *core* molecular formulae with the SPE-DOC concentrations in each sample to estimate the concentration of conserved DOC present in the global ocean (Figure 6b).

While molecular formulae from each group were present both in the surface and at depth, the estimated concentration of the *core* group was ~6–9 μM higher in warm surface waters (defined as those waters in subtropical and equatorial regions above 50 m depth, based on temperature; Figure 7a; Table 2) than the deep waters for each respective ocean basin (Table 2; Figures 6b and 7a). Moreover, the *core* SPE-DOC concentration in surface waters in the subpolar regions or Southern Ocean was not enhanced (Table 2; Figures 6b and 7). In fact, the concentration of the *core* in surface waters (Figure 7) correlated with temperature (Figures S3 and S4 in Supporting Information S1; $R^2 = 0.6$, $p < 0.0001$), implying that warmer surface waters contain more of the conservative fraction of DOM than colder surface waters.

The accumulation of the *core* group of molecular formulae in warm subtropical and equatorial surface waters highlights the importance of the low-latitude, warm regions in forming DOM that persists in the deep ocean.

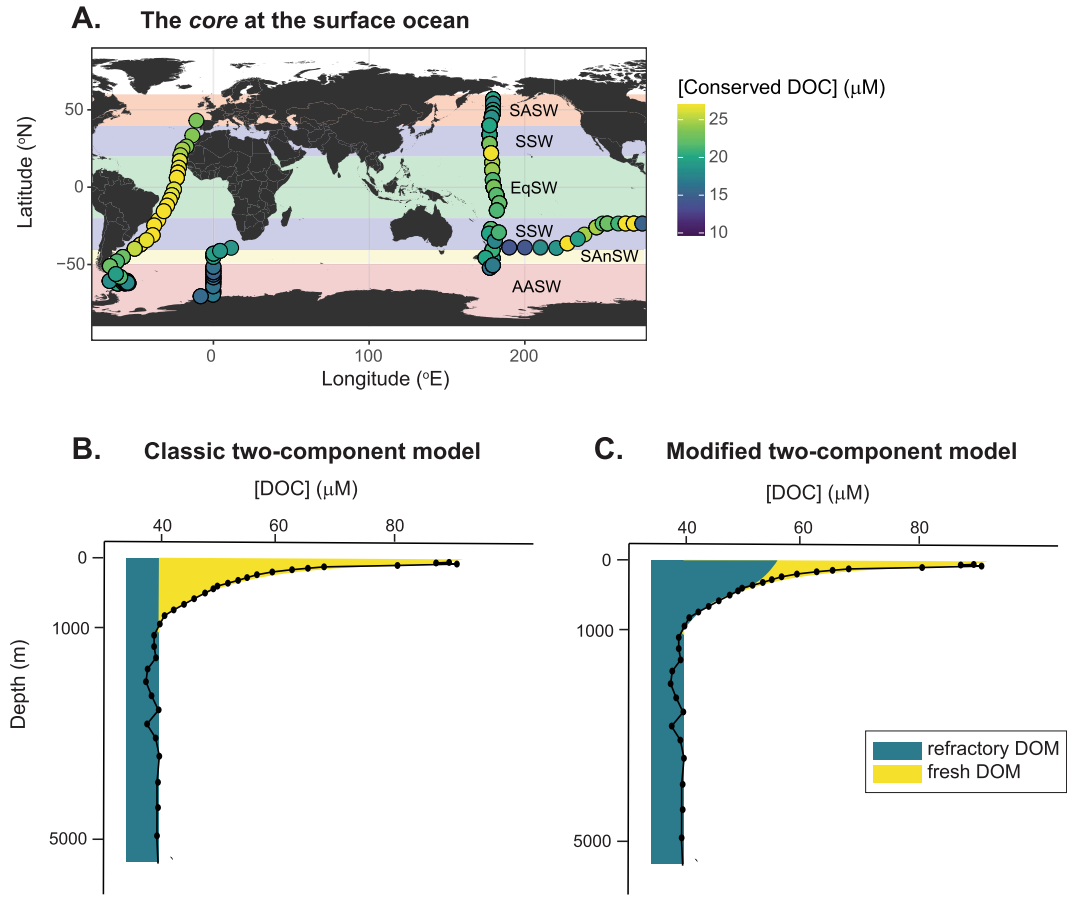

Figure 7. (a) Global map of the concentration of conserved DOC (calculated from the proportion of *core* molecular formulae) in warm surface waters (defined as depths shallower than 50 m). Definitions of the surface water masses (separated based on latitude and outlined in color) are as follows: SASW is Subarctic Surface Water, SSW is Subtropical Surface Water, EqSW is Equatorial Surface Water, SAnSW is Subantarctic Surface Water, and AASW is Antarctic Surface Water. SASW is defined as surface waters with latitude >40°N, respectively, SSW is between 20 and 40°N and S, respectively, EqSW is between 20°N and 20°S, and SAnSW is between 40°S and 50°S, and AASW is >50°S (beyond the Polar Front). These surface water distinctions are defined based on Talley (2011). (b) Classic two-component model (Hansell, 2013). (c) Modified two-component model in the low latitude ocean, when considering that the "core" is formed in the surface ocean. DOC concentration profile here is from CLIVAR cruise A16 at 10°N (Hansell et al., 2021).

Antarctic surface waters, on the other hand, had similar concentrations of conserved DOC (concentration of the *core*; Table 2; Figure 7) as deep waters (Figure 6b). Carlson et al. (1998) reported a similar result when comparing DOM from a phytoplankton bloom in the subtropical North Atlantic versus a bloom in the Ross Sea (Antarctica) and found that the DOM from the Ross Sea was more labile than that of the Atlantic. Temperature therefore likely plays an important role in regulating the formation of recalcitrant DOM, likely due to its effect on microbial activity. Temperature is a controlling factor in a microbial population (Ratkowsky et al., 1982), and warmer temperatures stimulate bacterial growth ((Barillier & Garnier, 1993; Kirchman & Rich, 1997)). Moreover, bacteria respond more slowly to a given substrate at colder temperatures (Kirchman & Rich, 1997). Warmer temperatures would therefore cause faster processing of fresh, recently produced organic matter and accumulation of more recalcitrant DOM. Nutrient depletion in warm, subtropical gyres also limits heterotrophic consumption of organic material (Thingstad et al., 1998) and thus more DOM may accumulate (Romera-Castillo et al., 2016). Interestingly, the core SPE-DOC concentration was elevated in our study in the oligotrophic gyres and equatorial upwelling regions alike, indicating that the observed elevated DOC concentration in the gyres is not solely related to the accumulation of recalcitrant DOM.

The classic two-component model, which is based on bulk $\Delta^{14}C$ values and DOC concentration profiles (Beaupre & Aluwihare, 2010; Williams & Druffel, 1987), describes a uniform refractory layer of DOM superimposed by a

Table 2
Mean (±Propagated Uncertainty) of Estimated DOC Concentrations (in μM) of the Core, New Source, Existing Source, and Sink Groups in the Major Deep Water Masses and Surface Waters

	Core	Existing source	New source	Sink
Atlantic				
NADW (13)	18 ± 3	3.0 ± 0.5	1.2 ± 0.7	2.9 ± 0.8
AABW (14)	17 ± 3	3.0 ± 0.6	1.6 ± 0.8	2.4 ± 0.9
SASW (1)	23	4	0.9	3.3
SSW (25)	26 ± 3	5 ± 0.6	1.9 ± 1.0	3.8 ± 1.0
EqSW (14)	26 ± 4	5 ± 0.7	1.6 ± 0.7	3.9 ± 1.1
SANSW (10)	20 ± 3	3 ± 0.5	1.5 ± 0.6	3.3 ± 0.9
AASW (59)	18 ± 2	3 ± 0.3	0.8 ± 0.2	3.6 ± 0.4
Pacific				
NPIW (29)	16 ± 3	0.7 ± 0.1	0.8 ± 0.5	3.2 ± 0.8
CDW (50)	16 ± 2	0.7 ± 0.1	0.8 ± 0.4	3.0 ± 0.5
PDW (19)	15 ± 2	0.7 ± 0.08	0.9 ± 0.4	2.8 ± 0.5
SASW (22)	20 ± 3	0.8 ± 0.1	1.3 ± 0.5	3.8 ± 0.7
SSW (49)	27 ± 9	1.1 ± 0.4	3 ± 4	4 ± 2
EqSW (40)	22 ± 5	0.9 ± 0.2	1.4 ± 0.5	3.8 ± 0.9
SANSW (8)	22 ± 5	0.9 ± 0.2	1.6 ± 0.8	4.1 ± 1
AASW (8)	19 ± 4	0.7 ± 0.1	1.2 ± 0.8	3.6 ± 1

Note. The number of samples for each water mass is given in parentheses. Water mass definitions are given in Figure 7 caption.

labile portion at the ocean's surface (Figure 7b). However, our molecular data indicate the refractory portion of DOM is not uniform but instead elevated at the surface compared to the deep (Figure 7c). Furthermore, there is clear latitudinal variability in the concentration of refractory SPE-DOC at the sea surface (Figure 7a). Similarly, Beaupre, Walker, & Druffel (2020) point out that the two-component model does not fully account for the complex biogeochemical processes that vary throughout the water column. Lewis, Walker, & Druffel (2021) likewise find that while refractory DOC concentrations are uniform in the deep ocean, they vary as a function of total DOC concentration in the surface ocean.

The DOC concentration of the *core* group in NADW is 18 ± 3 μM (Table 2). This concentration does not change until the deep waters reach the surface in the Southern Ocean and Antarctic Shelf Systems (Figure 6b). Once it reaches the Southern Ocean, NADW is introduced into the lower CDW fraction, which reaches depths as shallow as ∼1,000 m in the open Southern Ocean (Orsi, Johnson, & Bullister, 1999) and wells up to the surface (depths <50 m) in Antarctic Shelf systems (Orsi & Wiederwohl, 2009; Orsi, Johnson, & Bullister, 1999). The concentration of the *core* group is slightly lower in AABW and CDW in the Atlantic and Pacific sectors of the Southern Ocean (Table 2). PDW, the result of CDW overturning in the far North Pacific, has the lowest SPE-DOC concentration of the *core* (Table 2). The upwelling of CDW in the far North Pacific encounters NPIW, which reaches up to 200 m and is influenced by a minor contribution of terrigenous DOM (Nakatsuka et al., 2004; Whitney, Crawford, & Harrison, 2005) and high respiration (evidenced by the high AOU; Figure 1b). Similar to the DOC deficit in PDW near its formation site reported by Hansell and Carlson (2013) here, we observe a deficit in the *core* SPE-DOC concentrations.

Our findings are different from the current paradigm of slow, continuous degradation of recalcitrant DOM in the deep ocean (Hansell, 2013). We found instead that regions of overturning, where water masses are exposed to the subsurface, act as a sink for conserved DOM. Consequently, the *core* SPE-DOC concentration remains constant in the deep ocean. Our findings are consistent with a modeling study, where the amount of preformed DOC in the ocean's interior could be explained without any major input or removal to the pool (Matsumoto, Tanioka, & Gilchrist, 2022). That study suggested that water mass formation sites are important in determining preformed DOC distributions. Likewise, here the DOC concentration of the *core* group changes only when exposed to the surface at areas of overturning (Figure 6b). On much longer time scales, processes in the continental crust may contribute to the turnover of recalcitrant DOM (Hawkes et al., 2015; Walter et al., 2018).

Different chemical and physical environments likely play a role in the removal of the *core* at the subsurface and surface ocean. Changes in environmental conditions in the mesopelagic and surface ocean with respect to sunlight, nutrient availability, temperature, pressure, and microbial community composition and activity all play a role in whether there is a measurable microbial uptake of DOM (Amano et al., 2022; Bercovici et al., 2021). Moreover, DOM that escapes remineralization in one environment can be removed in short timescales when exposed to light and differing microbial communities, or mixed with more bioavailable DOM (Shen and Benner, 2018). The productive surface ocean has different microbial communities (Acinas et al., 2021) that are an order of magnitude higher in abundance than in the deep ocean (De Corte et al., 2012). Priming, or mixing recalcitrant DOM with a more labile substrate (Bianchi, 2012) when the deep waters reach surface depths, could also enhance the uptake and consumption of the *core* DOM. Microbes below the mixed layer in the Sargasso Sea consumed DOM that was recalcitrant to those microbes from the surface layer (Carlson, Ducklow, & Michaels, 1994). Likewise, microbes in the mesopelagic South Pacific gyre consumed DOM that accumulated in the upper mixed layer (Letscher et al., 2015). Enhanced DOM that remained for years in deep Antarctic shelf waters was remineralized upon export into AABW (Bercovici et al., 2017). Moreover, distinct turnover times of DOM can be explained by concentration-driven uptake and microbial interactions (Dittmar et al., 2021; Mentges et al., 2020). Furthermore, inputs of DOM from the surface may increase the concentration of individual compounds in the *core* group

above a threshold, thus rendering them available for microbial utilization (Arrieta et al., 2015a, 2015b; Bercovici et al., 2021). Our results support this previous work, in that while the *core* fraction of DOM remains untouched in the deep ocean for mixing timescales (~300 years in the Atlantic, ~500 years in the Pacific (Stuiver, Quay, & Ostlund, 1983); it can undergo modifications once it reaches the surface.

4.4. Dynamic Behavior of DOM in the Global Ocean

As with the *core* DOM, we calculated the apparent SPE-DOC concentrations of the *sources* and *sink* groups using their relative FT-ICR-MS signal proportions and bulk SPE-DOC concentrations (Table 2). There were <1–5 μM of the *new* and *existing source* groups and 3–5 μM of the *sink* group, regardless of ocean basin, depth, or water mass. The concentration of the *existing source* group (4 μM) was higher in the subtropical surface waters in the Atlantic compared to other oceanographic regions, suggesting that this group is also produced in the subtropical surface ocean. Oxidized components of DOM predominant in the *sink* group are preferentially removed by sorption, even at low concentrations (Avneri-Katz et al., 2017). Moreover, marine microgels in the open ocean spontaneously assemble via carboxyl group interactions, and the *sink* group has a higher O/H ratio (Table 1). The *sink* group could therefore be important for microgel formation in the open ocean. Once adsorbed onto a particle or assembled into a microgel, recalcitrant DOM may be more accessible to marine microbes and thus more susceptible to remineralization, or it may sink to the sediments. While the overall apparent radiocarbon age of DOC in pore waters is young (Bauer et al., 1995), 3%–8% of the total benthic DOC flux is recalcitrant and depleted in ^{14}C (Komada et al., 2013), suggesting that a portion of the particle flux contains recalcitrant DOM that has aged in the water column (Burdige & Komada, 2015).

The *new source* group showed an unexpected pattern in the deep Atlantic Ocean. SPE-DOC concentrations of this group were almost 4-fold higher from surface to depth at ~10 to 20°S in the Atlantic compared to any other site. At the same location, increased microbial activity at the surface was reported for the same cruise ((Dlugosch et al., 2022); Figure 8). Particle export events cause an increase in mesopelagic bacterial abundance and productivity (Hansell & Ducklow, 2003; Nagata et al., 2000; Yokokawa et al., 2013). The Brazil-Malvinas Confluence zone in this region is a hot spot for primary production (Goncalves-Araujo et al., 2012) and a major atmospheric carbon sink (Chiessi et al., 2007). Particles produced from primary production sink and release DOM. Lopez et al. (Lopez & Hansell, 2021) likewise found fresh, particle-derived DOC introduced into the ocean's interior at transition zones between fronts. The increased concentrations of the *new source* group therefore could be the residue of solubilized particles from a transient particle export event.

However, the concentrations of the *new source* group apart from this one region were comparably constant and low (<1 μM; Figure 8). In a back-of-the-envelope calculation, the concentration of individual molecular formulae in that group was estimated by dividing the apparent SPE-DOC concentration of this group (<1 μM; Table 2; Figure S3 in Supporting Information S1) by the number of *new source* molecular formulae (~2800; Table 1). This estimate results in a concentration of ~300 pM (10^{-12} M) of individual molecular formulae. As each molecular formulae in DOM contains many isomers, the concentration of individual compounds is far smaller (Seidel et al., 2022; Zark, Christoffers, & Dittmar 2017). The picomolar concentrations of individual molecular formulae

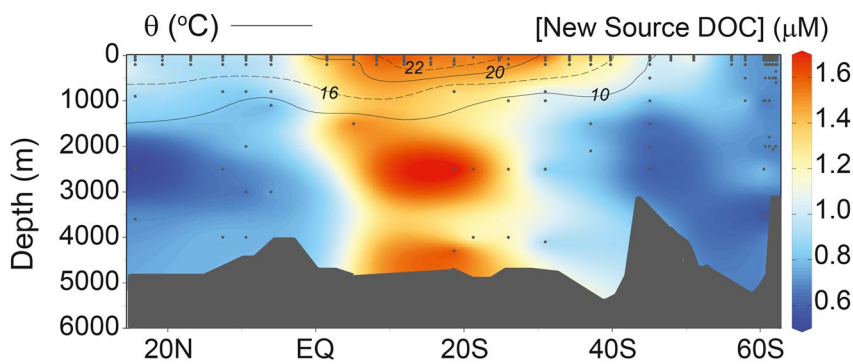

Figure 8. Concentration of *new source* SPE-DOC concentrations across the Atlantic (section outlined in Figure 2), with surface temperature in contours. Section was plotted using Ocean Data View (Schlitzer, 2023).

within this group are much smaller than the estimated concentrations (nanomolar) of the individual molecular formulae in the *existing source* and *sink* groups. Low concentrations may therefore limit the immediate complete removal of the *new source* group from the water column (Dittmar et al., 2021).

Moreover, while the DOM compositions of the *existing source* and *sink* groups were uniform across ocean basins, the composition of the *new source* group was variable and dynamic on the timescale of ocean mixing. The composition of the *new source* varied in neighboring samples of the same deep water mass that differ in age only by decades. Furthermore, we neither observed accumulation of the *new source* group nor traces of it downstream from areas where it was elevated (Figure 8). This pool of DOM is therefore transient and likely acts as a bioavailable substrate to microbial communities at depth. This explanation is supported by its relatively labile molecular composition (Figures 3c and 3d; Figure 5).

5. Conclusions

The two-endmember mixing analysis of bulk DOC and SPE-DOC concentrations revealed that both behave conservatively in the deep Atlantic and Pacific oceans. This finding contrasts with the current paradigm of slow, continuous degradation of recalcitrant DOM in the deep ocean (Hansell, 2013). We found instead that regions of overturning, where water masses are exposed to the subsurface, act as a sink for conserved DOM.

Likewise, the same mixing analysis with the thousands of identified constituents in marine DOM revealed that ~70% of its molecular composition follows the model with >99% confidence. As the *core* of conservatively mixing compounds comprises 14–20 μM of the SPE-DOC concentration in all deep samples, simple mixing is a major control on the molecular composition and distribution of DOM in the deep ocean. We conclude that changes in the molecular composition of DOM associated with the aging of deep water masses are a result of mixing of differential compositions of the endmembers and not a result of continuous degradation in the deep ocean.

Even though the largest part of DOM behaved conservatively in the deep ocean, 30% of its composition showed more dynamic behavior. These DOM constituents were added and removed relative to deep mixing and had distinct chemical properties. While the *source* and *sink* groups are present everywhere in the deep ocean, the *new source* is present at 4-fold higher concentrations in the south equatorial Atlantic, localized near the Brazil-Malvinas confluence zone. We infer solubilization of sinking particles as a likely reason behind this pattern, as evidenced by the high surface temperatures and elevated microbial activity in that region (Dlugosch et al., 2022), and the enhanced activity and solubilization of exported particles in a frontal convergence zone (Lopez & Hansell, 2021). Everywhere else, the *new source* group is at concentrations of ≤1 μM, indicating that the observed elevated concentrations of the *new source* are transient. The identification and characterization of dynamic fractions in deep ocean DOM, which on a bulk level follows conservative mixing, is consistent with scenarios of deep ocean microbial activity, solubilization from and adsorption to sinking particles.

Finally, our molecular data indicate that recalcitrant DOM (the *core*) is formed and accumulates in the surface ocean. Factors such as temperature, nutrient availability, differing microbial community composition and activity, and priming in the surface ocean play an important role in regulating the *core* distribution in the deep ocean. This work therefore illustrates the importance of the surface ocean in regulating DOM cycling and long-term organic carbon sequestration in the deep ocean.

Data Availability Statement

All data from this work is open access at PANGAEA Data Publisher at the following link: https://doi.org/10.1594/PANGAEA.962747.

Acknowledgments
We thank the scientific party and crew of cruises ANT28-2, 4 and 5, SO245, SO248, and SO254, and HOTS and BATS. We thank Helena Osterholz for DOM sample collection of SO245, Maren Wiemers for sample collection on ANT28-2, 4 and 5, Beatriz Noriega Ortega for sample collection on SO248 and SO254, and Aron Stubbins, Natasha McDonald and John Casey for collection of the BATS and HOTS samples. We additionally thank Ina Ulber, Matthias Friebe, Helena Osterholz and Katrin Klaproth for help with sample preparation and FT-ICR-MS analyses. Funding was provided by Deutsche Forschungsgemeinschaft (DFG) within the Collaborative Research Center Roseobacter (TRR 51). Open Access funding enabled and organized by Projekt DEAL.

References

Acinas, S. G., Sanchez, P., Salazar, G., Cornejo-Castillo, F. M., Sebastian, M., Logares, R., et al. (2021). Deep ocean metagenomes provide insight into the metabolic architecture of bathypelagic microbial communities. *Communications Biology*, *4*(1), 604. https://doi.org/10.1038/s42003-021-02112-2

Amano, C., Zhao, Z. H., Sintes, E., Reinthaler, T., Stefanschitz, J., Kisadur, M., et al. (2022). Limited carbon cycling due to high-pressure effects on the deep-sea microbiome. *Nature Geoscience*, *15*(12), 1041–1047. https://doi.org/10.1038/s41561-022-01081-3

Amon, R. M. W., & Benner, R. (1996). Bacterial utilization of different size classes of dissolved organic matter. *Limnology & Oceanography*, *41*(1), 41–51. https://doi.org/10.4319/lo.1996.41.1.0041

Arrieta, J. M., Mayol, E., Hansman, R. L., Herndl, G. J., Dittmar, T., & Duarte, C. M. (2015a). 'Dilution limits dissolved organic carbon utilization in the deep ocean. *Science*, *348*(6232), 331–333. https://doi.org/10.1126/science.1258955

Arrieta, J. M., Mayol, E., Hansman, R. L., Herndl, G. J., Dittmar, T., & Duarte, C. M. (2015b). Response to Comment on "Dilution limits dissolved organic carbon utilization in the deep ocean". *Science*, 350.

Avneri-Katz, S., Young, R. B., McKenna, A. M., Chen, H., Corilo, Y. E., Polubesova, T., et al. (2017). Adsorptive fractionation of dissolved organic matter (DOM) by mineral soil: Macroscale approach and molecular insight. *Organic Geochemistry*, *103*, 113–124. https://doi.org/10.1016/j.orggeochem.2016.11.004

Barillier, A., & Garnier, J. (1993). Influence of temperature and substrate concentration on bacterial-growth yield in seine river water batch cultures. *Applied and Environmental Microbiology*, *59*(5), 1678–1682. https://doi.org/10.1128/aem.59.5.1678-1682.1993

Bauer, J. E., Reimers, C. E., Druffel, E. R. M., & Williams, P. M. (1995). Isotopic constraints on carbon exchange between deep-ocean sediments and sea-water. *Nature*, *373*(6516), 686–689. https://doi.org/10.1038/373686a0

Beaupre, S. R., & Aluwihare, L. (2010). Constraining the 2-component model of marine dissolved organic radiocarbon. *Deep Sea Research Part II: Topical Studies in Oceanography*, *57*(16), 1494–1503. https://doi.org/10.1016/j.dsr2.2010.02.017

Beaupre, S. R., Walker, B. D., & Druffel, E. R. M. (2020). The two-component model coincidence: Evaluating the validity of marine dissolved organic radiocarbon as a stable-conservative tracer at Station M. *Deep Sea Research Part II: Topical Studies in Oceanography*, *173*, 104737. https://doi.org/10.1016/j.dsr2.2020.104737

Benner, R., Biddanda, B., Black, B., & McCarthy, M. (1997). Abundance, size distribution, and stable carbon and nitrogen isotopic compositions of marine organic matter isolated by tangential-flow ultrafiltration. *Marine Chemistry*, *57*(3–4), 243–263. https://doi.org/10.1016/s0304-4203(97)00013-3

Bercovici, S., Dittmar, T., & Niggemann, J. (2023). Dissolved organic matter molecular composition data and supporting metadata for multiple oceanographic cruises with RV SONNE (SO254, SO245, SO248) and RV POLARSTERN (PS79), Bermuda Atlantic Time-series Study and Hawaii Ocean Time-series. *PANGAEA*.

Bercovici, S. K., Arroyo, M. C., De Corte, D., Yokokawa, T., & Hansell, D. A. (2021). Limited utilization of extracted dissolved organic matter by prokaryotic communities from the subtropical North Atlantic. *Limnology & Oceanography*, *66*(6), 2509–2520. https://doi.org/10.1002/lno.11769

Bercovici, S. K., & Hansell, D. A. (2016). Dissolved organic carbon in the deep Southern Ocean: Local versus distant controls. *Global Biogeochemical Cycles*, *30*(2), 350–360. https://doi.org/10.1002/2015gb005252

Bercovici, S. K., Huber, B. A., DeJong, H. B., Dunbar, R. B., & Hansell, D. A. (2017). Dissolved organic carbon in the Ross Sea: Deep enrichment and export. *Limnology & Oceanography*, *62*(6), 2593–2603. https://doi.org/10.1002/lno.10592

Bercovici, S. K., Koch, B. P., Lechtenfeld, O. J., McCallister, S. L., Schmitt-Kopplin, P., & Hansell, D. A. (2018). Aging and molecular changes of dissolved organic matter between two deep oceanic end-members. *Global Biogeochemical Cycles*, *32*(10), 1449–1456. https://doi.org/10.1029/2017gb005854

Bercovici, S. K., McNichol, A. P., Xu, L., & Hansell, D. A. (2018). Radiocarbon content of dissolved organic carbon in the South Indian Ocean. *Geophysical Research Letters*, *45*(2), 872–879. https://doi.org/10.1002/2017gl076295

Bianchi, T. S. (2012). The role of terrestrially derived organic carbon in the coastal ocean: A changing paradigm and the priming effect (vol 108, pg 19473, 2011). *Proceedings of the National Academy of Sciences of the United States of America*, *109*.

Broek, T. A. B., Walker, B. D., Guilderson, T. P., & McCarthy, M. D. (2017). Coupled ultrafiltration and solid phase extraction approach for the targeted study of semi-labile high molecular weight and refractory low molecular weight dissolved organic matter. *Marine Chemistry*, *194*, 146–157. https://doi.org/10.1016/j.marchem.2017.06.007

Broek, T. A. B., Walker, B. D., Guilderson, T. P., Vaughn, J. S., Mason, H. E., & McCarthy, M. D. (2020). Low molecular weight dissolved organic carbon: Aging, compositional changes, and selective utilization during global ocean circulation. *Global Biogeochemical Cycles*, *34*(6). https://doi.org/10.1029/2020gb006547

Burdige, D. J., & Komada, T. (2015). "Sediment pore waters," biogeochemistry of marine dissolved organic matter (2nd ed., pp. 535–577).

Carlson, C. A., & Ducklow, H. W. (1996). Growth of bacterioplankton and consumption of dissolved organic carbon in the Sargasso Sea. *Aquatic Microbial Ecology*, *10*, 69–85. https://doi.org/10.3354/ame010069

Carlson, C. A., Ducklow, H. W., Hansell, D. A., & Smith, W. O. (1998). Organic carbon partitioning during spring phytoplankton blooms in the Ross Sea polynya and the Sargasso Sea. *Limnology & Oceanography*, *43*(3), 375–386. https://doi.org/10.4319/lo.1998.43.3.0375

Carlson, C. A., Ducklow, H. W., & Michaels, A. F. (1994). Annual flux of dissolved organic-carbon from the Euphotic zone in the Northwestern Sargasso Sea. *Nature*, *371*(6496), 405–408. https://doi.org/10.1038/371405a0

Chiessi, C. M., Ulrich, S., Mulitza, S., Patzold, J., & Wefer, G. (2007). Signature of the Brazil-Malvinas Confluence (Argentine Basin) in the isotopic composition of planktonic foraminifera from surface sediments. *Marine Micropaleontology*, *64*(1–2), 52–66. https://doi.org/10.1016/j.marmicro.2007.02.002

D'Andrilli, J., Cooper, W. T., Foreman, C. M., & Marshall, A. G. (2015). An ultrahigh-resolution mass spectrometry index to estimate natural organic matter lability. *Rapid Communications in Mass Spectrometry*, *29*(24), 2385–2401. https://doi.org/10.1002/rcm.7400

De Corte, D., Sintes, E., Yokokawa, T., Reinthaler, T., & Herndl, G. J. (2012). Links between viruses and prokaryotes throughout the water column along a North Atlantic latitudinal transect. *ISME Journal*, *6*(8), 1566–1577. https://doi.org/10.1038/ismej.2011.214

Dittmar, T., Koch, B., Hertkorn, N., & Kattner, G. (2008). A simple and efficient method for the solid-phase extraction of dissolved organic matter (SPE-DOM) from seawater. *Limnology and Oceanography: Methods*, *6*, 230–235. https://doi.org/10.4319/lom.2008.6.230

Dittmar, T., Lennartz, S. T., Buck-Wiese, H., Hansel, D. A., Santinelli, C., Vanni, C., et al. (2021). Enigmatic persistence of dissolved organic matter in the ocean. *Nature Reviews Earth & Environment*, *2*(8), 570–583. https://doi.org/10.1038/s43017-021-00183-7

Dlugosch, L., Poehlein, A., Wemheuer, B., Pfeiffer, B., Badewien, T. H., Daniel, R., & Simon, M. (2022). Significance of gene variants for the functional biogeography of the near-surface Atlantic Ocean microbiome. *Nature Communications*, *13*(1), 456. https://doi.org/10.1038/s41467-022-28128-8

Druffel, E. R. M., & Griffin, S. (2015). Radiocarbon in dissolved organic carbon of the South Pacific Ocean. *Geophysical Research Letters*, *42*(10), 4096–4101. https://doi.org/10.1002/2015gl063764

Druffel, E. R. M., Griffin, S., Coppola, A. I., & Walker, B. D. (2016). Radiocarbon in dissolved organic carbon of the Atlantic Ocean. *Geophysical Research Letters*, *43*(10), 5279–5286. https://doi.org/10.1002/2016gl068746

Druffel, E. R. M., Griffin, S., Lewis, C. B., Rudresh, M., Garcia, N. G., Key, R. M., et al. (2021). Dissolved organic radiocarbon in the Eastern Pacific and southern oceans. *Geophysical Research Letters*, *48*(10), e2021GL092904. https://doi.org/10.1029/2021gl092904

Flerus, R., Lechtenfeld, O. J., Koch, B. P., McCallister, S. L., Schmitt-Kopplin, P., Benner, R., et al. (2012). A molecular perspective on the ageing of marine dissolved organic matter. *Biogeosciences*, *9*(6), 1935–1955. https://doi.org/10.5194/bg-9-1935-2012

Follett, C. L., Repeta, D. J., Rothman, D. H., Xu, L., & Santinelli, C. (2014). Hidden cycle of dissolved organic carbon in the deep ocean. *Proceedings of the National Academy of Sciences of the United States of America*, *111*(47), 16706–16711. https://doi.org/10.1073/pnas.1407445111

Fontela, M., Garcia-Ibanez, M. I., Hansell, D. A., Mercier, H., & Perez, F. F. (2016). Dissolved organic carbon in the North Atlantic meridional overturning circulation. *Scientific Reports*, *6*(1), 26931. https://doi.org/10.1038/srep26931

Fontela, M., Perez, F. F., Mercier, H., & Lherminier, P. (2020). North Atlantic western boundary currents are intense dissolved organic carbon streams. *Frontiers in Marine Science*, *7*. https://doi.org/10.3389/fmars.2020.593757

Goncalves-Araujo, R., De Souza, M. S., Mendes, C. R. B., Tavano, V. M., Pollery, R. C., & Garcia, C. A. E. (2012). Brazil-Malvinas confluence: Effects of environmental variability on phytoplankton community structure. *Journal of Plankton Research*, *34*(5), 399–415. https://doi.org/10.1093/plankt/fbs013

Green, N. W., Perdue, E. M., Aiken, G. R., Butler, K. D., Chen, H. M., Dittmar, T., et al. (2014). An intercomparison of three methods for the large-scale isolation of oceanic dissolved organic matter. *Marine Chemistry*, *161*, 14–19. https://doi.org/10.1016/j.marchem.2014.01.012

Hansell, D. A. (2013). Recalcitrant dissolved organic carbon fractions. *Annual Review of Marine Science*, *5*(5), 421–445. https://doi.org/10.1146/annurev-marine-120710-100757

Hansell, D. A., & Carlson, C. A. (1998). Deep-ocean gradients in the concentration of dissolved organic carbon. *Nature*, *395*(6699), 263–266. https://doi.org/10.1038/26200

Hansell, D. A., & Carlson, C. A. (2013). Localized refractory dissolved organic carbon sinks in the deep ocean. *Global Biogeochemical Cycles*, *27*(3), 705–710. https://doi.org/10.1002/gbc.20067

Hansell, D. A., Carlson, C. A., Amon, R. M. W., Álvarez-Salgado, X. A., Yamashita, Y., Romera-Castillo, C., & Bif, M. B. (2021). In *Compilation of dissolved organic matter (DOM) data obtained from the global ocean surveys from 1994 to 2021 (NCEI Accession 0227166)*. NOAA National Centers for Environmental Information.

Hansell, D. A., Carlson, C. A., Repeta, D. J., & Schlitzer, R. (2009). Dissolved organic matter in the ocean a controversy stimulates new insights. *Oceanography*, *22*(4), 202–211. https://doi.org/10.5670/oceanog.2009.109

Hansell, D. A., & Ducklow, H. W. (2003). Bacterioplankton distribution and production in the bathypelagic ocean: Directly coupled to particulate organic carbon export? *Limnology & Oceanography*, *48*(1), 150–156. https://doi.org/10.4319/lo.2003.48.1.0150

Hansell, D. A., & Orellana, M. V. (2021). Dissolved organic matter in the global ocean: A primer. *Gels*, *7*(3), 128. https://doi.org/10.3390/gels7030128

Hansman, R. L., Dittmar, T., & Herndl, G. J. (2015). Conservation of dissolved organic matter molecular composition during mixing of the deep water masses of the northeast Atlantic Ocean. *Marine Chemistry*, *177*, 288–297. https://doi.org/10.1016/j.marchem.2015.06.001

Hansman, R. L., Griffin, S., Watson, J. T., Druffel, E. R. M., Ingalls, A. E., Pearson, A., & Aluwihare, L. I. (2009). The radiocarbon signature of microorganisms in the mesopelagic ocean. *Proceedings of the National Academy of Sciences of the United States of America*, *106*(16), 6513–6518. https://doi.org/10.1073/pnas.0810871106

Hawkes, J. A., Rossel, P. E., Stubbins, A., Butterfield, D., Connelly, D. P., Achterberg, E. P., et al. (2015). 'Efficient removal of recalcitrant deep-ocean dissolved organic matter during hydrothermal circulation. *Nature Geoscience*, *8*(11), 856–860. https://doi.org/10.1038/ngeo2543

Hertkorn, N., Benner, R., Frommberger, M., Schmitt-Kopplin, P., Witt, M., Kaiser, K., et al. (2006). 'Characterization of a major refractory component of marine dissolved organic matter. *Geochimica et Cosmochimica Acta*, *70*(12), 2990–3010. https://doi.org/10.1016/j.gca.2006.03.021

Jiao, N. Z., Herndl, G. J., Hansell, D. A., Benner, R., Kattner, G., Wilhelm, S. W., et al. (2011). 'The microbial carbon pump and the oceanic recalcitrant dissolved organic matter pool. *Nature Reviews Microbiology*, *9*(7), 555. https://doi.org/10.1038/nrmicro2386-c5

Kirchman, D. L., & Rich, J. H. (1997). Regulation of bacterial growth rates by dissolved organic carbon and temperature in the equatorial Pacific Ocean. *Microbial Ecology*, *33*(1), 11–20. https://doi.org/10.1007/s002489900003

Koch, B. P., & Dittmar, T. (2006). From mass to structure: An aromaticity index for high-resolution mass data of natural organic matter. *Rapid Communications in Mass Spectrometry*, *20*(5), 926–932. https://doi.org/10.1002/rcm.2386

Komada, T., Burdige, D. J., Crispo, S. M., Druffel, E. R. M., Griffin, S., Johnson, L., & Le, D. (2013). Dissolved organic carbon dynamics in anaerobic sediments of the Santa Monica Basin. *Geochimica et Cosmochimica Acta*, *110*, 253–273. https://doi.org/10.1016/j.gca.2013.02.017

Lechtenfeld, O. J., Kattner, G., Flerus, R., McCallister, S. L., Schmitt-Kopplin, P., & Koch, B. P. (2014). Molecular transformation and degradation of refractory dissolved organic matter in the Atlantic and Southern Ocean. *Geochimica et Cosmochimica Acta*, *126*, 321–337. https://doi.org/10.1016/j.gca.2013.11.009

Letscher, R. T., Knapp, A. N., James, A. K., Carlson, C. A., Santoro, A. E., & Hansell, D. A. (2015). Microbial community composition and nitrogen availability influence DOC remineralization in the South Pacific Gyre. *Marine Chemistry*, *177*, 325–334. https://doi.org/10.1016/j.marchem.2015.06.024

Lewis, C. B., Walker, B. D., & Druffel, E. R. M. (2021). New radiocarbon constraints on the global cycling of solid-phase extractable dissolved organic carbon. *Geophysical Research Letters*, *48*(14), e2020GL090995. https://doi.org/10.1029/2020gl090995

Lopez, C. N., & Hansell, D. A. (2021). Evidence of deep DOC enrichment via particle export beneath subarctic and northern subtropical fronts in the North Pacific. *Frontiers in Marine Science*, *8*. https://doi.org/10.3389/fmars.2021.659034

Matsumoto, K., Tanioka, T., & Gilchrist, M. (2022). Sensitivity of steady state, deep ocean dissolved organic carbon to surface boundary conditions. *Global Biogeochemical Cycles*, *36*(1), e2021GB007102. https://doi.org/10.1029/2021gb007102

Medeiros, P. M., Seidel, M., Powers, L. C., Dittmar, T., Hansell, D. A., & Miller, W. L. (2015). Dissolved organic matter composition and photochemical transformations in the northern North Pacific Ocean. *Geophysical Research Letters*, *42*(3), 863–870. https://doi.org/10.1002/2014gl062663

Mentges, A., Deutsch, C., Feenders, C., Lennartz, S. T., Blasius, B., & Dittmar, T. (2020). Microbial physiology governs the oceanic distribution of dissolved organic carbon in a scenario of equal degradability. *Frontiers in Marine Science*, *7*. https://doi.org/10.3389/fmars.2020.549784

Mentges, A., Feenders, C., Seibt, M., Blasius, B., & Dittmar, T. (2017). Functional molecular diversity of marine dissolved organic matter is reduced during degradation. *Frontiers in Marine Science*, *4*. https://doi.org/10.3389/fmars.2017.00194

Merder, J., Freund, J. A., Feudel, U., Hansen, C. T., Hawkes, J. A., Jacob, B., et al. (2020). ICBM-OCEAN: Processing ultrahigh-resolution mass spectrometry data of complex molecular mixtures. *Analytical Chemistry*, *92*(10), 6832–6838. https://doi.org/10.1021/acs.analchem.9b05659

Nagata, T., Fukuda, H., Fukuda, R., & Koike, I. (2000). Bacterioplankton distribution and production in deep Pacific waters: Large-scale geographic variations and possible coupling with sinking particle fluxes. *Limnology & Oceanography*, *45*(2), 426–435. https://doi.org/10.4319/lo.2000.45.2.0426

Nakatsuka, T., Toda, M., Kawamura, K., & Wakatsuchi, M. (2004). Dissolved and particulate organic carbon in the Sea of Okhotsk: Transport from continental shelf to ocean interior. *Journal of Geophysical Research*, *109*(C9), C09S14. https://doi.org/10.1029/2003jc001909

Orsi, A. H., Johnson, G. C., & Bullister, J. L. (1999). Circulation, mixing, and production of Antarctic bottom water. *Progress in Oceanography*, *43*(1), 55–109. https://doi.org/10.1016/s0079-6611(99)00004-x

Orsi, A. H., & Wiederwohl, C. L. (2009). A recount of Ross Sea waters. *Deep Sea Research Part II: Topical Studies in Oceanography*, *56*(13–14), 778–795. https://doi.org/10.1016/j.dsr2.2008.10.033

Osterholz, H., Kilgour, D. P. A., Storey, D. S., Lavik, G., Ferdelman, T. G., Niggemann, J., & Dittmar, T. (2021). Accumulation of DOC in the South Pacific subtropical Gyre from a molecular perspective. *Marine Chemistry*, *231*, 103955. https://doi.org/10.1016/j.marchem.2021.103955

Ratkowsky, D. A., Olley, J., Mcmeekin, T. A., & Ball, A. (1982). Relationship between temperature and growth-rate of bacterial cultures. *Journal of Bacteriology*, *149*, 1–5. https://doi.org/10.1128/jb.149.1.1-5.1982

R Core Team. (2022). *R: A language and environment for statistical computing*. R Foundation for Statistical Computing. URL Retrieved from https://www.R-project.org/

Romera-Castillo, C., Letscher, R. T., & Hansell, D. A. (2016). New nutrients exert fundamental control on dissolved organic carbon accumulation in the surface Atlantic Ocean. *Proceedings of the National Academy of Sciences of the United States of America*, *113*(38), 10497–10502. https://doi.org/10.1073/pnas.1605344113

Schlitzer, R. (2023). Ocean Data View. Retrieved from https://odv.awi.de

Schmidt, F., Elvert, M., Koch, B. P., Witt, M., & Hinrichs, K. U. (2009). Molecular characterization of dissolved organic matter in pore water of continental shelf sediments. *Geochimica et Cosmochimica Acta*, *73*(11), 3337–3358. https://doi.org/10.1016/j.gca.2009.03.008

Schmitz, W. J. (1995). On the interbasin-scale thermohaline circulation. *Reviews of Geophysics*, *33*(2), 151–173. https://doi.org/10.1029/95rg00879

Seidel, M., Vemulapalli, S. P. B., Mathieu, D., & Dittmar, T. (2022). Marine dissolved organic matter shares thousands of molecular formulae yet differs structurally across major water masses. *Environmental Science & Technology*, *56*(6), 3758–3769. https://doi.org/10.1021/acs.est.1c04566

Seidel, M., Yager, P. L., Ward, N. D., Carpenter, E. J., Gomes, H. R., Krusche, A. V., et al. (2015). Molecular-level changes of dissolved organic matter along the Amazon River-to-ocean continuum. *Marine Chemistry*, *177*, 218–231. https://doi.org/10.1016/j.marchem.2015.06.019

Shen, Y., & Benner, R. (2018). Mixing it up in the ocean carbon cycle and the removal of refractory dissolved organic carbon. *Scientific Reports*, *8*(1), 2542. https://doi.org/10.1038/s41598-018-20857-5

Stuiver, M., Quay, P. D., & Ostlund, H. G. (1983). Abyssal water C-14 distribution and the age of the world oceans. *Science*, *219*(4586), 849–851. https://doi.org/10.1126/science.219.4586.849

Talley, L. D. (2011). *Descriptive physical oceanography an introduction*. Academic Press.

Talley, L. D. (2013). Closure of the global overturning circulation through the Indian, Pacific, and southern oceans: Schematics and transports. *Oceanography*, *26*(1), 80–97. https://doi.org/10.5670/oceanog.2013.07

Thingstad, T. F., Zweifel, U. L., & Rassoulzadegan, F. (1998). P limitation of heterotrophic bacteria and phytoplankton in the northwest Mediterranean. *Limnology & Oceanography*, *43*(1), 88–94. https://doi.org/10.4319/lo.1998.43.1.0088

Verdugo, P. (2004). The role of marine gel-phase on carbon cycling in the ocean. *Marine Chemistry*, *92*(1–4), 65–66. https://doi.org/10.1016/j.marchem.2004.06.037

Walker, B. D., Primeau, F. W., Beaupre, S. R., Guilderson, T. P., Druffel, E. R. M., & McCarthy, M. D. (2016). Linked changes in marine dissolved organic carbon molecular size and radiocarbon age. *Geophysical Research Letters*, *43*(19), 10385–10393. https://doi.org/10.1002/2016gl070359

Walter, S. R. S., Jaekel, U., Osterholz, H., Fisher, A. T., Huber, J. A., Pearson, A., et al. (2018). Microbial decomposition of marine dissolved organic matter in cool oceanic crust. *Nature Geoscience*, *11*(5), 334–339. https://doi.org/10.1038/s41561-018-0109-5

Whitney, F. A., Crawford, W. R., & Harrison, P. (2005). Physical processes that enhance nutrient transport and primary productivity in the coastal and open ocean of the subarctic NE Pacific. *Deep Sea Research Part II: Topical Studies in Oceanography*, *52*(5–6), 681–706. https://doi.org/10.1016/j.dsr2.2004.12.023

Williams, P. M., & Druffel, E. R. M. (1987). Radiocarbon in dissolved organic-matter in the central North Pacific-Ocean. *Nature*, *330*(6145), 246–248. https://doi.org/10.1038/330246a0

Yokokawa, T., Yang, Y. H., Motegi, C., & Nagata, T. (2013). Large-scale geographical variation in prokaryotic abundance and production in meso- and bathypelagic zones of the central Pacific and Southern Ocean. *Limnology & Oceanography*, *58*(1), 61–73. https://doi.org/10.4319/lo.2013.58.1.0061

Zark, M., Christoffers, J., & Dittmar, T. (2017). Molecular properties of deep-sea dissolved organic matter are predictable by the central limit theorem: Evidence from tandem FT-ICR-MS. *Marine Chemistry*, *191*, 9–15. https://doi.org/10.1016/j.marchem.2017.02.005

Zark, M., & Dittmar, T. (2018). Universal molecular structures in natural dissolved organic matter. *Nature Communications*, *9*(1), 3178. https://doi.org/10.1038/s41467-018-05665-9

Zigah, P. K., McNichol, A. P., Xu, L., Johnson, C., Santinelli, C., Karl, D. M., & Repeta, D. J. (2017). Allochthonous sources and dynamic cycling of ocean dissolved organic carbon revealed by carbon isotopes. *Geophysical Research Letters*, *44*(5), 2407–2415. https://doi.org/10.1002/2016gl071348